Journal of Catalysis **212,** 182–192 (2002)
doi:10.1006/jcat.2002.3786

On the Performance of Porous Vycor Membranes for Conversion Enhancement in the Dehydrogenation of Methylcyclohexane to Toluene

P. Ferreira-Aparicio,*,[1] I. Rodriguez-Ramos,* and A. Guerrero-Ruiz†

**Instituto de Catálisis y Petroleoquímica, CSIC, Campus de Cantoblanco, E-28049 Madrid, Spain; and †Dpto. de Química Inorgánica y Técnica, UNED, C/Senda del Rey, s/n, E-28040 Madrid, Spain*

Received April 29, 2002; revised August 5, 2002; accepted August 7, 2002

Some parameters influencing methylcyclohexane dehydrogenation over a Pt/Al_2O_3 catalyst using a porous Vycor membrane reactor are evaluated. For the Vycor membrane H_2 separation factors with respect to methylcyclohexane (MCH) and toluene (TOL) have been found to be above the values predicted by the Knudsen diffusion model. By adjusting the experimental conditions to equilibrate the H_2 production and the extraction rates, an enhancement of the net performance of the system is achieved. For an adequate ratio between the reactant fed flow and the membrane surface area, the extraction conditions used can improve the yield. Thus, the increase in the purge gas flow rate and the countercurrent operation mode favour the equilibrium shift by increasing the H_2 and TOL partial pressures difference between both sides of the membrane and decreasing that of MCH. The distribution of the catalytic zone is also important. The membrane efficiency can be optimised if the reactant mixture reaches the catalyst in the porous zone under the equilibrium conditions achieved in a conventional fixed-bed reactor.

Key Words: **hydrogen; methylcyclohexane; toluene; membrane reactor; porous Vycor; Pt/Al_2O_3.**

1. INTRODUCTION

Although hydrogen is not a primary energy form, it can be used as an energy carrier through which other primary energy sources can be transmitted and utilised (1–4). The main problem for the use of hydrogen is the difficulty in creating of a distribution infrastructure for safe and cost-effective transport and storage. Storage methods currently used are too expensive and do not meet the performance requirements of future applications (5). New technologies will need to be developed on the basis of production and storage systems that come into use as the hydrogen economy advances.

Some of the proposed methods consist of H_2 production by reforming of liquid compounds such as methanol or gasoline. However, these are not long-term solutions, as they are not zero-contaminant emission processes. Methanol is the easiest liquid to reform but it raises health-and-safety and industrial-liability concerns, as it is classified as a toxin and has an invisible flame when burned. Furthermore, methanol would require changes in the gasoline distribution and storage infrastructure, changes that might not justify the investment if methanol is an intermediate step to hydrogen (1, 6). Zero-emission systems require the development of reversible hydrogen storage processes. There are several possibilities for hydrogen storage: in the form of liquid H_2; as gaseous hydrogen at high pressure; in the form of metallic hydrides; by adsorption in carbon nanotubes, graphite nanofibers, or glass microspheres; or in the form of organic hydrides (5–10). This last option, in which reversible chemical reactions are used to incorporate gaseous hydrogen into a liquid compound from which it can be released again by dehydrogenation, seems to be one of the alternatives that could be introduced on a local scale under economically acceptable conditions (1, 10–12). The use of compounds such as toluene (TOL), which can store hydrogen with a specific volume of 46 kg H_2/m^3 in the form of methylcyclohexane (MCH), has been already shown to be potentially feasible for both mobile and stationary applications (11, 13). There are also some aspects related to this form of storage to take into consideration in contrast to other alternatives: MCH is a liquid at ambient pressure and temperature and, given that its consistence and specific weight are very similar to the crude oil, it can be stored and transported in existing oil tanks and ships. Thus, it could be a more attractive option to be adopted in the medium term in view of a smooth energy system infrastructure transition.

This reversible reaction of dehydrogenation of MCH to TOL, and in general all dehydrogenation reactions of paraffins to aromatic compounds, is highly endothermic and strongly limited by thermodynamic equilibrium (14). The removal of one of the reaction products by an appropriate membrane would cause a shift in the equilibrium conditions

---

[1] To whom correspondence should be addressed. Fax: +34 91 585 4760. E-mail: pferreira@icp.csic.es.

0021-9517/02 $35.00

and a conversion enhancement, allowing operation at lower temperatures and increasing system efficiency (15).

Previous work dedicated to membrane reactor application to this or other related processes by using palladium and palladium alloy-based membranes, alumina fibers, and porous glass can be found in the literature (16–24). However, many more fundamental studies are needed to develop a MTH system (methylcyclohexane–toluene–hydrogen) operating under optimal conditions, which could be applied as a hydrogen storage-production system. In this paper we report a study on the applicability of porous Vycor glass membranes to the conversion enhancement of the dehydrogenation of MCH to TOL. We do not attempt to study a system operating under experimental conditions that would require a practical application. Our objective is to determine those parameters that have a major influence on the operation efficiency of this system as compared to a conventional catalytic reactor and to establish the basis for the future design of an efficient reactor–separator to obtain high yields at low temperatures. The coupling of a catalytic reactor and a extractor in the same unit is an attractive concept, but its operation involves an extremely complex mechanism in which a great variety of parameters must be taken into account: for instance, the reactant feed rate, the influence of the removal rate of permeated species, the direction of the permeated flow compared to that of the reactant, the amount and distribution of the catalyst, the thermal gradients in the catalytic bed, and the ratio between the volume of gas and the membrane surface. This paper will try to shed some light on some of these aspects.

2. EXPERIMENTAL

A Pt/Al_2O_3 catalyst was used to study the MCH dehydrogenation reaction. It was prepared by incipient wetness impregnation of an Al_2O_3 support (Degussa, $S_{B.E.T.} = 180\ m^2/g$) with an aqueous solution of H_2PtCl_6 (Aldrich). After impregnation it was dried overnight and calcined in air at 773 K for 3 h. The metal loading in the sample was exactly determined by chemical analysis. The platinum dispersion was calculated from the H_2 uptake on the reduced sample. Volumetric H_2 chemisorption measurements were carried out at room temperature after reduction of the sample in H_2 atmosphere at 673 K for 2 h. Details of the preparation of this catalyst can be found elsewhere (25).

Vycor glass membranes were prepared from long porous Vycor glass tubes (Corning) (26). The outer diameter of the cylindrical pieces is 10 mm with a 1-mm wall thickness. According to the manufacturer specifications the pore size of this material is 4 nm and its specific surface area is $250\ m^2 \cdot g^{-1}$. The permeation zone was reduced to a 4-cm-long central section by sintering both sides of the tube at high temperature using very low heating and cooling rates. The method used to eliminate the porosity of the material was checked to be effective by preparing a completely impervious tube, which was tested for several hours in a pressurised closed system without showing any leak. The tube was assembled in the membrane reactor by fitting its ends to a glass shell by means of glass threads with silicon joints. The membrane zone had a volume of $2.01\ cm^3$ and a porous surface area of $10.05\ cm^2$. The outer tube was equipped with a gas inlet and outlet, which allowed the use of a sweep gas to remove the permeated species.

A scheme of the experimental setup for reaction and permeability tests is presented in Fig. 1. The Vycor permeability was measured for pure gases (H_2, He, N_2) as a function of the transmembrane pressure. In order to determine the separation factor of MCH and TOL with respect to H_2, a gas mixture with H_2 : MCH : He in proportions (5.8 : 4.7 : 89.5) or with MCH : TOL : He in proportions (4.7 : 3.2 : 92.1) was fed into the tube side at a flow rate of $0.134\ mol \cdot h^{-1}$, while a pure He stream was passed by the shell side at the same molar flow rate. The final composition of each gas mixture flowing by the tube side and the shell side was determined by gas chromatographic analysis using a TCD detector.

For reaction tests the catalyst was reduced at 673 K for 2 h under pure H_2 fed at a flow rate of $0.054\ mol \cdot h^{-1}$. After reduction the reactor was flushed with He and cooled to the reaction temperature. The reactant mixture was fed by saturating a He flow in liquid MCH (Panreac, 99% purity), which was maintained in an isothermal bath at 293 K. The saturated gas was a mixture of 4.7% in a volume of MCH in He. Initially, some reaction experiments were performed in a fixed-bed reactor with different catalyst loads in order to determine the activity of the catalyst under differential conditions, its stability at different temperatures, and the maximum conversion for the system. Theoretical values for equilibrium conversion, as predicted by Thermodynamics, were also calculated, according to the stoichiometry of the reaction from the Gibbs free energy values of each component at several temperatures.

Experiments with the membrane reactor were carried out with an excess of catalyst in order to ensure reaching those thermodynamic equilibrium conditions. Usually 1 g of catalyst (0.42- to 0.59-mm particle size) was loaded inside the Vycor tube along the porous zone. A thermocouple inside the membrane allowed a determination of the temperature in the central part of the catalytic bed. The furnace was controlled by a second thermocouple located at its inner wall. A He stream fed at the shell side was used as sweeping gas for the permeated especies. Gases flowing by each side of the membrane reactor were analysed both together and separately (tube side and shell side) to determine the net performance of the system and the distribution of species at both sides of the membrane tube. Some reaction tests were also carried out under the same conditions in the nonextracting operation mode by substituting the Vycor membrane with an impervious glass tube.

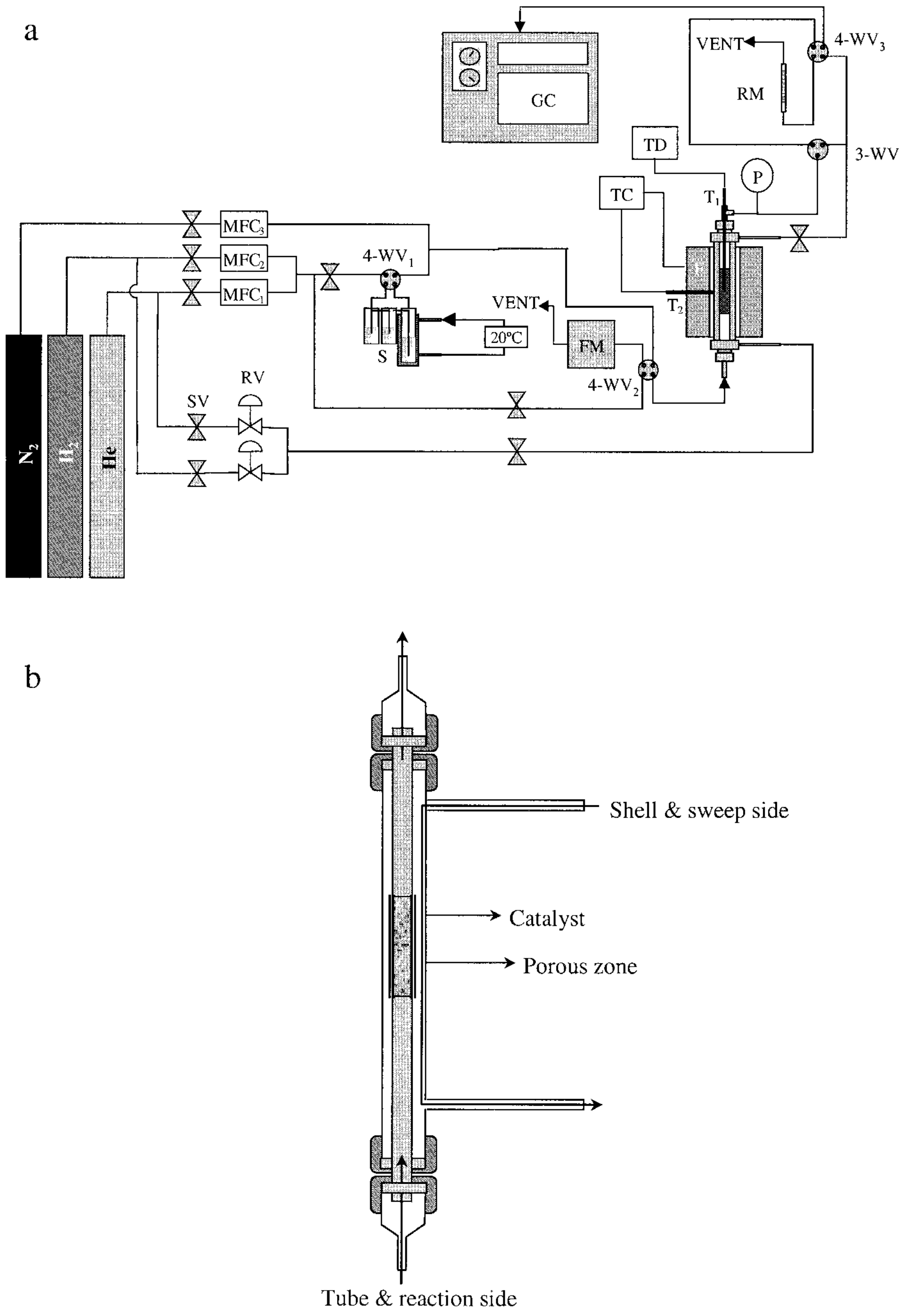

FIG. 1. (a) Experimental setup for permeability measurements and reaction tests. (F) furnace, (FM) flow meter, (GC) gas chromatograph, (MFC) mass flow controllers, (P) pressure meter, (RM) rotar meter, (RV) regulation valves, (S) saturator, (SV) on/off valves, (T_1) catalytic bed thermocouple, (T_2) furnace control thermocouple, (TC) temperature controller, (TD) temperature display, (3-WV) three way valve, (4-WV) four-way valve. (b) Detail of the membrane reactor.

3. RESULTS AND DISCUSSION

The Pt/Al_2O_3 catalyst used had a metal content of 0.83 wt%. The high H_2 uptake obtained by chemisorption (32.9 $\mu mol \cdot g^{-1}$) indicates a good metal dispersion in the support (78%). A Pt average particle size in the catalyst of 1.5 nm has been estimated from the H_2 adsorption measurements by assuming the formation of spherical particles, whose surface is constituted by equal proportions of those planes of lower Miller indexes (27).

Initial reaction tests, carried out under differential conditions in a nonmembrane configuration, allowed a determination of the catalytic activity and stability of the Pt/Al_2O_3 sample for the methylcyclohexane dehydrogenation reaction. Catalytic activity values of 1.6 and 6.3 $\mu mol \cdot g^{-1} \cdot s^{-1}$ were obtained at 473 and 523 K, respectively. The Pt/Al_2O_3

catalyst showed good stability at those temperatures, and no deactivation was observed for about 24 h. No side reactions were observed and only hydrogen and toluene (TOL) were obtained as reaction products. At higher temperatures (673 K) the catalyst suffered a pronounced deactivation and lost its activity completely after a few minutes as a result of the fast MCH decomposition and the formation of coke on its surface. A similar behaviour has been recently found on mono- and bimetallic platinum catalysts supported on alumina for the cyclohexane dehydrogenation reaction (28). For these kinds of catalysts the dehydrogenation activity does not improve or even decline beyond 623 K due to a stronger adsorption of the aromatic compound that retards further cyclohexane adsorption and reaction and favours its decomposition to form graphitic carbon. In agreement with this results, on Al_2O_3-supported Pt–Au catalysts it has also been shown that the methylcyclohexane dehydrogenation takes place along with the formation of benzene and other cracking products at temperatures above 673 K, leading to deactivation processes (29).

Equilibrium conversion values for the reaction were calculated as a function of the temperature for the conditions that would be later experimentally used to carry out the reaction tests. The equilibrium constant was determined for the reaction at each temperature from the Gibbs free energy values of reactants and products at different temperatures (30). According to the stoichiometry of the dehydrogenation reaction ($MCH \Leftrightarrow TOL + 3H_2$) the equilibrium conversion was estimated from the equilibrium constant values. Given the fact that for reaction tests the reactant was fed by saturating a He flow in liquid MCH maintained at 293 K, the theoretical conversion level, presented in Fig. 2, was calculated for the MCH vapour pressure at that temperature (4.8 kPa). On the basis of these data, for a given MCH partial pressure (p_{MCH}) of 0.047 at 101.3 kPa total pressure in the system, the dehydrogenation reaction proceeds at temperatures above 373 K and reaches conversion levels higher than 99% at temperatures above 523 K. Experimental values obtained for the Pt/Al_2O_3 catalyst under equilibrium conditions in a tubular fixed-bed reactor are also presented in the same figure for comparison purposes. Both theoretical and experimental data show a relative good agreement when the nonisothermal operation of the reactor and the difficulty in controlling the temperature all along the catalytic bed is considered. This kind of reaction, highly endothermic, generally causes large temperature gradients in packed-bed reactors. Some attempts to improve the heat transfer to the catalyst by using wall reactors to carry out the methylcyclohexane dehydrogenation can be found in the literature (31).

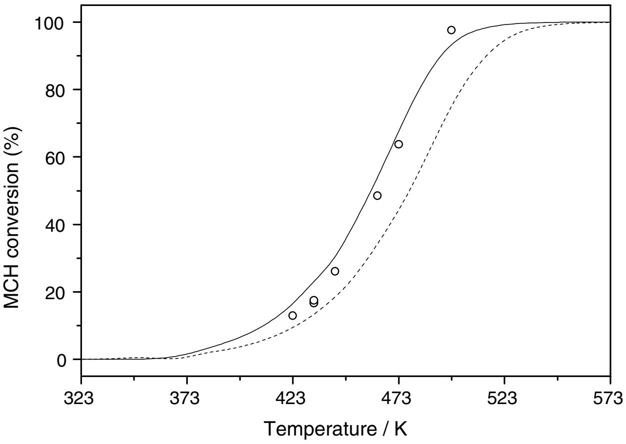

FIG. 2. MCH conversion values for its dehydrogenation at atmospheric pressure as a function of the reaction temperature. (Circles) Experimental data points for 0.047 MCH partial pressure. (Solid line) Theoretical values for 0.047 MCH partial pressure. (Dotted line) Theoretical values for 0.1 MCH partial pressure.

The effect of increasing the MCH partial pressure in the feed stream was also theoretically evaluated. By raising p_{MCH} to 0.1, higher temperatures, exceeding 543 K, are needed to reach conversion levels higher than 99%, as shown in Fig. 2. Given the fact that in the course of the reaction there is an increment in the number of moles in the system corresponding to $3x$, where x is the number of moles of MCH converted, for a given temperature an increase in pressure will give place to a lower conversion, an obvious consequence of Le Chatelier's principle. The equilibrium conversion values obtained at higher system pressures have also been theoretically estimated for $p_{MCH} = 0.047$ at constant temperature (453 K). An increment from atmospheric pressure (101.3 kPa) up to 170.2 kPa would suppose a diminishing in MCH conversion from 41.5 to 29.1%. Taking into account these calculations, the conditions chosen to carry out the MCH dehydrogenation tests in the membrane reactor were atmospheric pressure and $p_{MCH} = 0.047$.

3.1. Vycor Permeability

Before reaction tests in the membrane reactor were initiated, some attempts to determine the Vycor properties for gas separation were carried out. Permeability of Vycor was measured for pure gases (H_2, He, and N_2) at different temperatures. Their permeance, defined as the ratio between the flux across the membrane and the pressure difference between both sides of the porous wall, was observed not to depend on the transmembrane pressure for the above-mentioned gases. On the contrary, it followed a linear relationship with the reciprocal of the square root of the molecular weight of different gases (H_2, He, CH_4, and N_2) (Fig. 3a). With regard to the temperature effect, gas permeance through the Vycor tube was also found to be inversely proportional to the square root of the absolute temperature, as is shown in Fig. 3b for H_2. The relationship observed between the permeance and parameters such as the transmembrane pressure, the molecular weight of the molecules, or the temperature indicates that the transport

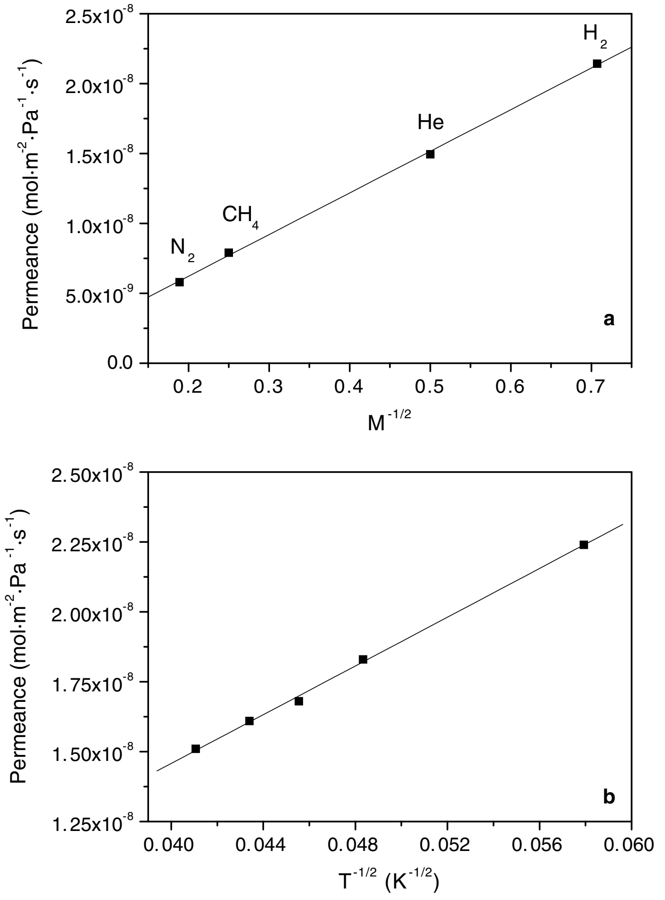

FIG. 3. (a) Permeance of single gases through Vycor glass at 298 K versus the reciprocal of their molecular masses square roots. (b) H_2 permeance through porous Vycor versus the reciprocal of the absolute temperature square root.

mechanism operating in the Vycor membrane for these light gases, H_2, He, CH_4, and N_2, is governed by Knudsen diffusion. According to it, permeance is proportional to the value of $(M \cdot T)^{-1/2}$, where M is the molecular weight of the permeated species and T is the system absolute temperature. The proportionality constant between them depends on the porosity, the tortuosity, and the thickness of the membrane. The experimentally determined H_2 permeability through Vycor glass in the present study (1.9×10^{-8} mol · m^{-2} · s^{-1} · Pa^{-1} at 530 K) is within the range of values reported in the literature for this material, which vary between 1.8 and 5.4×10^{-8} mol · m^{-2} · s^{-1} · Pa^{-1} (32–34). However, by considering the fact that the temperatures at which those values have been measured are higher (873 K), a slightly lower permeability has been obtained in our Vycor membrane. From data in Ref. (32), a reference value for H_2 permeance can be interpolated at 530 K which corresponds to 4.2×10^{-8} mol · m^{-2} · s^{-1} · Pa^{-1}. The lower permeance obtained in our case could be due to a smaller pore size in the transition region dividing the porous and the impervious zones in the tube.

Ideal separation factors, calculated as a measure of the preferential separation of one species compared to another, are compiled in Table 1. They have been obtained as the quotient of permeances for two single gases. The separation factors of H_2 with reference to MCH and TOL were experimentally determined by analysing the permeated amounts of each compound through the Vycor membrane from H_2 : MCH : He and MCH : TOL : He gas mixtures. The ideal Knudsen separation factor of a species i in comparison to a species j has been estimated from the ratio between the square root of the molecular masses of the respective compounds i and j according to

$$\alpha_{ij} = \sqrt{M_j}/\sqrt{M_i}. \qquad [1]$$

The excellent agreement between the experimentally determined values for the light gases H_2, He, and N_2 and those theoretically calculated also corroborates the above-proposed transport mechanism. On the other hand, a higher separation factor has been found for H_2 than for TOL and, in particular, for MCH with reference to the Knudsen predicted values. This deviation of the experimental data from those theoretically calculated indicates an interaction of these organic compounds with the porous structure of the membrane walls that impedes their diffusion in comparison to gases such as H_2, He, and N_2 and favours their separation. It must be considered that permselectivities for lighter gases have been calculated from the permeance of single gases, whereas the values for MCH and TOL were obtained by a different method. This latter estimation, using gas chromatography to determine the permeated amounts from mixtures of the different compounds involved in the reaction (H_2, MCH, TOL), gives more realistic data regarding the permeation process that takes place under reaction conditions. However, a strict comparison with the rest of values determined from permeances of single gases could be inadequate. According to the gas chromatographic analysis of the permeated amounts, a permeance value of 3.46×10^{-8} mol · m^{-2} · s^{-1} · Pa^{-1} has been measured for H_2 by using a purge flow rate of 0.134 mol · h^{-1}, almost twice as high as for the single-gas permeation experiments. For MCH and TOL the measured permeation rates

TABLE 1

Separation Factors for Gases through the Vycor Membrane at 523 K

i/j	α_{ij} (experimental)	Knudsen α_{ij}
H_2/N_2	3.9	3.74
H_2/CH_4	2.9	2.83
H_2/He	1.5	1.41
H_2/C_7H_{14}	15.4	7.00
H_2/C_7H_8	7.9	6.78
C_7H_8/C_7H_{14}	2.0	1.03

correspond to 2.24 and 4.47×10^{-9} $\mathrm{mol\cdot m^{-2}\cdot s^{-1}\cdot Pa^{-1}}$, respectively.

3.2. Membrane Reactor Tests

Tests on the membrane reactor showed an improvement in the conversion for the MCH dehydrogenation reaction, which was largely dependent on the experimental conditions. By feeding the reactant mixture at a molar flow rate of 1.34×10^{-2} $\mathrm{mol\cdot h^{-1}}$ (gas hourly space velocity (GHSV: 150 $\mathrm{h^{-1}}$) and the sweep gas at the same flow rate in the countercurrent mode, a level of conversion of 45% was initially obtained. The temperature in the catalytic bed was 453 K. For those conditions, thermodynamics predicts a conversion of 41.5%. The MCH percentage converted to TOL continued increasing slowly with time and after 6 h reached a constant level close to 65%. The evolution along with time of the distribution of MCH and TOL at the tube side in the membrane reactor at 453 K is presented in Fig. 4. The permeance of the different species through the Vycor glass, the progressive change of their concentration profiles along the catalytic bed, and the subsequent conversion increase are probably the reasons for this extended time for gas composition equilibration on both sides of the membrane.

3.2.1. Effect of the reactant feed flow rate. By considering the fact that one of the parameters controlling the effectiveness of a membrane for the preferential removal of H_2 will depend on the ratio between the flow feed at the reaction side (F_R) and the porous surface in the membrane (S_p), the effect of this parameter on conversion was examined. Figure 5 shows a plot of the MCH converted as a function of the F_R value for a constant sweep gas flow rate of 2.68×10^{-2} $\mathrm{mol\cdot h^{-1}}$ and a given S_p (10.05 $\mathrm{cm^2}$). By reducing the reactant feed rate the equilibrium is shifted towards the dehydrogenation reaction and the conversion is enhanced. Because of the low permeance of the Vycor membrane, a higher porous surface with reference to the reactant mixture flow favours the direct process of dehydrogenation by preferential separation of the reaction products, in particular H_2. By increasing the contact time between the volume of gas in the reaction side and the permeation zone, the separation efficiency is improved. No significant temperature variation was observed when the reactant feed flow was changed. The temperature in the catalytic bed was observed to oscillate between 453 and 449 K for the lowest and highest feed flow rates, respectively. Furthermore, for high F_R values, above 6×10^{-2} $\mathrm{mol\cdot h^{-1}}$, the catalyst mass is the factor that limits kinetically the reactor performance.

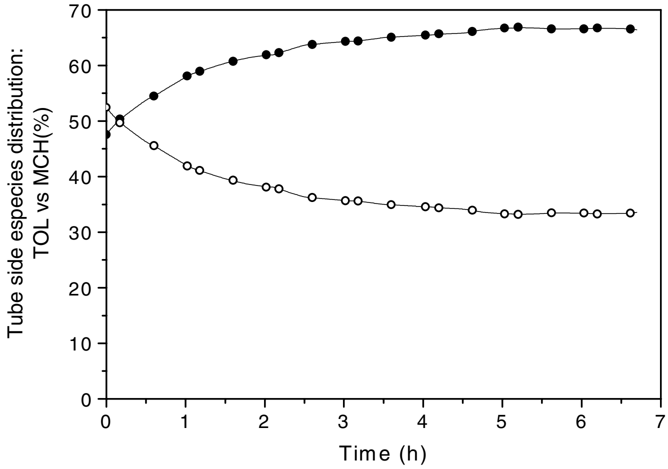

FIG. 4. Evolution with time of the relative amounts of methylcyclohexane (MCH) (○) and toluene (TOL) (●) at the membrane reaction side. Reaction conditions: feed flow rate, 1.34×10^{-2} $\mathrm{mol\cdot h^{-1}}$; sweep gas flow rate, 1.34×10^{-2} $\mathrm{mol\cdot h^{-1}}$; catalytic bed temperature (T_1), 453 K. MCH partial pressure, 0.047. Theoretical equilibrium conversion at 453 K, 41.5%.

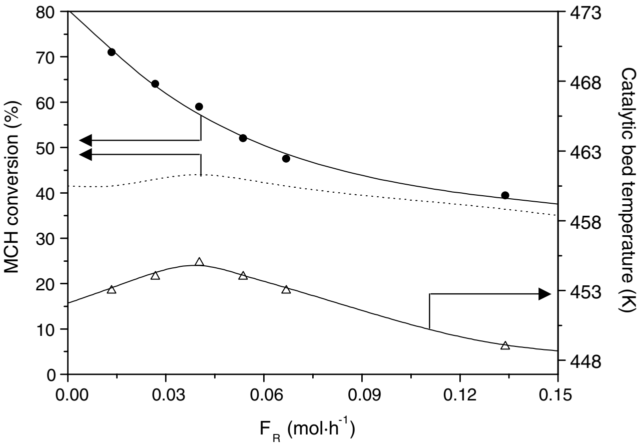

FIG. 5. MCH conversion in the membrane reactor versus the reactant flow rate (F_R) (●). Theoretical conversion values corresponding to the catalytic bed temperature (· · ·). (Right axis) Catalytic bed temperature (Δ). Membrane porous surface area (S_p), 10.05 $\mathrm{cm^2}$. MCH partial pressure, 0.047. Sweep gas flow rate, 2.68×10^{-2} $\mathrm{mol\cdot h^{-1}}$.

In order to explore the effect that the reactant feed flow rate exerts in the operation of a fixed-bed reactor for this dehydrogenation process with a high reaction enthalpy, the membrane was replaced with an impervious glass tube. A certain conversion enhancement could also be observed by reducing the GHSV of the reactant mixture, as shown in Fig. 6, although it was not as relevant as in the case of the reactor operating with the Vycor membrane. In addition, the catalytic bed temperature was detected to increase from 458 to 470 K when reducing the molar flow rate from 29.64×10^{-2} to 5.4×10^{-3} $\mathrm{mol\cdot h^{-1}}$. If the experimentally determined data for conversion are compared with the thermodynamic predicted values for the equilibrium conversion at the temperature measured in the catalytic bed, a perfect agreement is found between them at F_R values below 6×10^{-2} $\mathrm{mol\cdot h^{-1}}$. For higher values the fed mixture cannot reach equilibrium conversions and becomes limited by the catalyst load. The effect of temperature variation

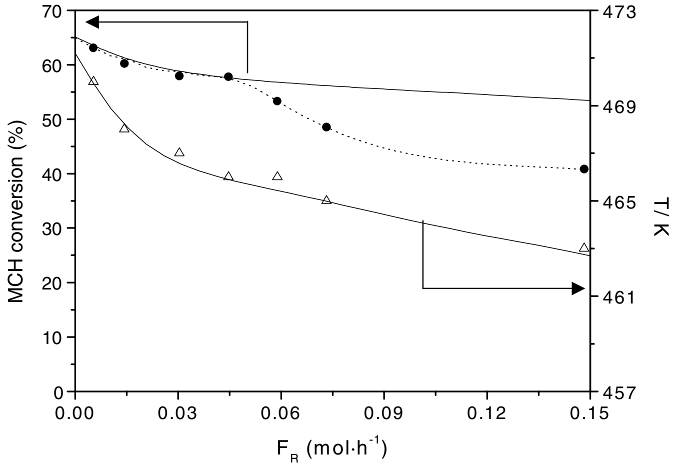

FIG. 6. MCH conversion in a fixed-bed reactor as a function of the reactant molar flow rate (F_R). (Left axis) Experimental data for MCH conversion (●) and theoretical conversion values for the measured temperature (—). (Right axis) Catalytic bed temperature experimentally measured versus the reactant flow rate (Δ). MCH partial pressure, 0.047. Note that temperatures in the catalytic bed are higher than those in the membrane reactor for the same furnace temperature (T_2).

with the reactant feed flow rate finds explanation in the highly endothermic nature of the reaction; i.e.,

$$C_7H_{14} \Leftrightarrow C_7H_8 + 3H_2, \quad \Delta H^o_{R(298\,K)} = 204\,kJ \cdot mol^{-1},$$

which contributes to the nonisothermal operation of the system and leads to changes in the temperature along the catalytic bed. These temperature changes have been observed and studied in the literature for this particular process and other related reactions, both in conventional (11, 13) and membrane reactors (16), with a finding that there is a temperature decrease at the entrance of the catalytic bed that becomes more pronounced when the space velocity is increased. The higher the reactant feed rate, the larger the catalyst fraction (or catalytic bed length) involved in the reaction progress. Given the fact that in the membrane reactor the preferential separation of the reaction products extends the catalytic bed length participating in the reaction progress, the temperature changes are reduced compared with that in the conventional fixed-bed reactor.

3.2.2. Effect of the extraction conditions. The extraction conditions also affected the reaction progress. The system efficiency improved when the gas flow rates in the permeation side were increased. The sweep flow variation from 1.34 to 107.14×10^{-2} mol · h^{-1} in the countercurrent mode with reference to the tube side enhanced the conversion and yielded higher TOL/MCH ratios in the reaction side flow. For higher flow rates, conversion was not improved and the TOL/MCH ratio decreased, as shown in Fig. 7. The improved yield obtained at high sweeping gas rates cannot be ascribed to a dilution effect, as indicated by CG analysis at the reaction side, but to a different permeance of the gases participating in the reaction, which is favoured by a more effective extraction. The maxima reached in the TOL/MCH ratio could be due to the relative proportion between the extraction and the reaction rates. For very high sweep gas flow rates the preferential extraction of the reaction products, which is responsible of the equilibrium shift, probably competes with the MCH extraction rate, which limits the reaction progress at the tube side. Therefore, when a larger proportion of MCH is permeated to the shell side, the TOL/MCH ratio decreases after reaching a maximum.

Based on the permeation measurements carried out for mixture with a H_2 partial pressure $p_{H_2} = 0.057$, a H_2 permeation flux of 7.2×10^{-4} mol · h^{-1} was obtained with a sweep stream of 13.39×10^{-2} mol · h^{-1}. Considering the theoretical MCH conversion for the conditions used (41.5%), for a feed flow rate of 13.39×10^{-2} mol · h^{-1} the rate of H_2 formation should be close to 7.8×10^{-3} mol · h^{-1}. Under these conditions approximately only one-tenth of the H_2 produced should be removed from the tube side. By reducing the feed rate to 1.34×10^{-2} mol · h^{-1} the rate of H_2 production would decrease to a level of 7.8×10^{-4} mol · h^{-1}, close to the permeation rate. The equilibration between both rates allows modifying the equilibrium conditions and increasing conversion.

Moon and Park reported recently a theoretical model to describe the effects of the permeability–selectivity pair on membrane reactors for a similar process: the dehydrogenation of cyclohexane to benzene (35). Based on this model, for a given permselectivity, the conversion can be expressed as a function of the Damkoehler and the Peclet numbers. The first one (D_a) depends linearly on the volume of the reaction side, the catalyst loading, the reaction rate constant,

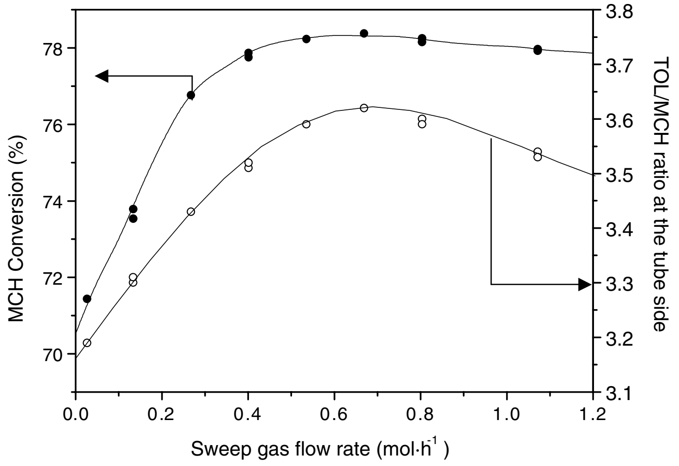

FIG. 7. Effect of the sweep gas flow rate on the membrane reactor performance. (Solid symbols (left axis)) MCH conversion as a function of the sweep gas flow rate. (Open symbols (right axis)) evolution of the toluene to methylcyclohexane ratio at the reaction side. The sweep gas is fed in the countercurrent mode. Reactant feed flow rate, 1.34×10^{-2} mol · h^{-1}. MCH partial pressure, 0.047. Reaction temperature, 453 K.

and the system total pressure and is inversely proportional to the reactant feed rate. On the other hand, the Peclet number (P_e) keeps a direct proportionality with the molar feed rate of the reactant and the inverse of the porous surface, the reactant permeance, and the total pressure in the system. The experimental results here obtained correlate well with the theoretical results given by Moon and Park. When D_a has very low values, the reaction kinetics controls conversion, which is independent of P_e. For larger D_a values there is a region controlled by selective permeation. Although there are optimum values of both parameters for reaching the best conditions for the system operation, in general a lower reactant feed rate leads to a decreased P_e and increased D_a, and enhances the reaction conversion. In our case, for low reactant feed rate, the Vycor membrane seems to be operating under a regime for which conversion is controlled by the preferential removal of the reaction products: mainly H_2, and in second place TOL, with reference to the reactant. As shown in Fig. 8, when the reactant feed rate is reduced and the system is operating at lower $\log(P_e)$ values ranging from 1.1 to 0.1 and higher $\log(D_a)$ from 6.7 to 7.7, MCH conversion is enhanced from 39 to 71%. By increasing the sweep gas flow rate, the permeance of the different species is favoured, resulting in lower P_e values, which also favours a higher conversion.

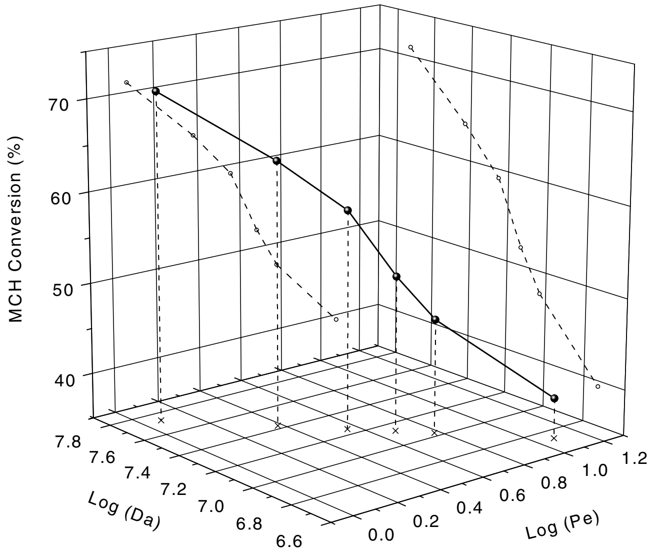

FIG. 8. Experimental MCH conversion plotted versus the logarithm of the Peclet (P_e) and Damkoehler (D_a) numbers (see Appendix). Projection over planes in dotted lines. Reaction temperature, 453 K.

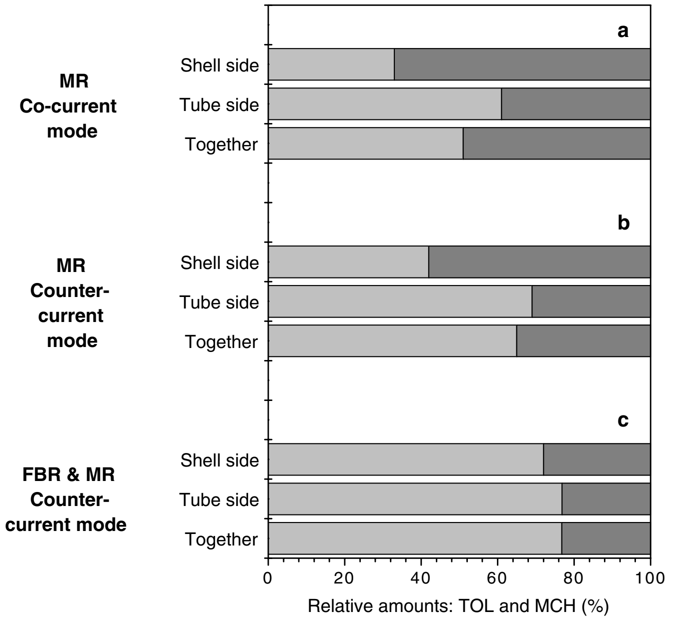

FIG. 9. Toluene (light gray) and methylcyclohexane (dark gray) distribution at the reaction side, at the shell side, and in the analysis of both streams together for the membrane reactor. (a) membrane reactor (Pt/Al_2O_3) operating in the cocurrent mode; (b) membrane reactor (Pt/Al_2O_3) operating in the countercurrent mode; (c) fixed-bed prereactor (Pt/Al_2O_3) and membrane reactor (Pt/Al_2O_3) operating in the countercurrent mode. Catalytic bed temperature, 453 K. Reactant flow rate, 1.34×10^{-2} mol · h^{-1}. Sweep gas flow rate, 1.34×10^{-2} mol · h^{-1}.

3.2.3. Effect of the sweep gas feed mode. The removal of species through the membrane was also conditioned by the direction of the feed gases flowing by the tube and shell sides in countercurrent (previously analysed) and cocurrent mode. For this last configuration, when the sweep gas flow was fed at 1.34×10^{-2} mol · h^{-1} in the same direction as the reactant mixture at the tube side (1.34×10^{-2} mol · h^{-1}), the extraction was less effective than in the countercurrent operation. However, an improvement in conversion related to the equilibrium conditions was also obtained. Figure 9 presents the relative percentage of TOL and MCH from the analysis of the reaction side and the shell side flows separately. The relative percentage of MCH and TOL for both streams together is also included in Fig. 9 and gives an indication of the net MCH conversion. The differences between these two different modes of operation can be clearly observed from Figs. 9a and 9b: a membrane reactor with the tube side and shell side gases flowing in the same direction (Fig. 9a) and a membrane reactor working in the countercurrent mode (Fig. 9b). In the countercurrent mode the extraction of products is favoured, in particular that of H_2, and conversion increases. The ratio H_2/TOL in the sweep gas at the shell side also revealed this difference. A much higher H_2/TOL value of 36 was determined in the sweep stream for the countercurrent mode, compared with a H_2/TOL of 29 found for the configuration with reactant and extractor flowing in the same direction. Although permeability measurements have shown that TOL is more easily permeated than MCH, under reaction conditions the sweep gas flow is preferentially enriched (apart from H_2) in MCH compared to that in TOL, which occurs in larger proportion at the tube side (Figs. 9a and 9b). This distribution

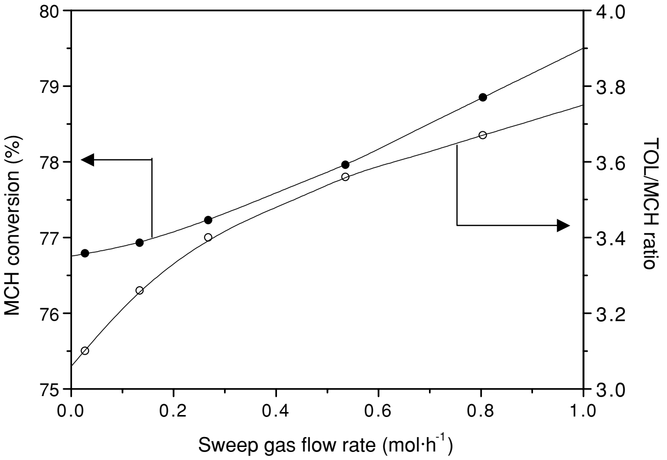

FIG. 10. Effect of the sweep gas flow rate on a system integrating a fixed-bed reactor in series with the membrane reactor. (Left axis) Methylcyclohexane conversion obtained as a function of the purge gas flow rate (solid symbols). (Right axis) Toluene-to-methylcyclohexane ratio (open symbols). Catalytic bed temperature, 453 K. Reactant flow rate, 1.34×10^{-2} mol · h^{-1}.

of species is the result of a permeation process taking place all along the porous zone, in which the reactant and products concentration profile varies with the distance from the frontal part of the catalytic bed. The higher concentration of MCH at the shell side in comparison to that of TOL can be ascribed to the higher permeation of MCH in the membrane zone, where the reaction has not reached the equilibrium conditions yet and the MCH concentration is higher that those of the reaction products.

In order to check this previous explanation, some tests were carried out by feeding the tube side of the membrane reactor with the outlet flow coming from a conventional fixed-bed reactor in series with it and maintained at the same temperature in the same furnace. This assembly allows the reaction mixture in the tube side to reach the catalytic bed along the porous zone in equilibrium. By using the same conditions as in the previous experiments (reactant and sweep gas flow rate, 1.34×10^{-2} mol · h^{-1}), the MCH conversion increased to 77% (Fig. 9c), compared with the 65% value reached in the absence of the prereactor (Fig. 9b). In this case the proportion of TOL in the shell side is considerably increased in relation to that of MCH (from 42 to 72%). Then, this difference is a consequence of the lower MCH concentration in the former part of the membrane reactor. By increasing the sweep gas flow rate to 80.36×10^{-2} mol · h^{-1} with this system configuration (Fig. 10), MCH conversion could be finally enhanced to 79%. In this case a further increase in the extracting gas flow continued favouring the progress of the dehydrogenation reaction due to the lower proportion of reactant lost by permeance to the shell side. A similar experiment related to the effect of catalyst packing was recently carried out by Kikuchi *et al.* with a Pd membrane (36). In concordance with our results, when the catalyst was packed, not only along the permeation zone but also extending it into the part before the membrane, enhanced hydrogen permeation and production was obtained. This configuration allows the whole permeating surface to operate under the most favourable conditions, for which the H_2 partial pressure is the maximum achievable. In our case, for a porous membrane in a membrane reactor, the presence of a prereactor allows the mixture in the reaction side to reach the porous zone under the thermodynamic equilibrium conditions, with the maximum partial pressure of products and the minimum partial pressure of reactant. By considering that the permeation driving force of a species i is its partial pressure difference between both sides of the membrane, a prereactor makes it possible to maximise the effectiveness of the system. This configuration not only enhances the permeation rate of products (H_2 and TOL) also decreases that of MCH compared with the conventional packing mode. This is also in line with the higher efficiency obtained in the countercurrent extraction mode than in the cocurrent sweep stream. The countercurrent operation establishes a higher partial pressure gradient for products between both sides of the membrane at the rear of the catalytic bed and favours in this way the progress of the reaction. With this configuration the TOL space–time yield obtained was 0.426 mol · h^{-1} · kg$_{\text{cat}}^{-1}$. Ciavarella *et al.* (37) drew parallel conclusions from their study on isobutane dehydrogenation, concluding that for the case of a countercurrent sweep stream the global performance of the reactor is limited by the catalyst activity, while for a cocurrent sweep mode performance is limited by the membrane selectivity.

The above-presented results indicate that a great variety of parameters influence the operation of a reactor–separator system. Among them we could mention the reactant feed rate, extracting conditions such as the flow rate of a sweep gas or its direction related to that of the reactant, and the permeance of the membrane and its selectivity. By considering the relationship between the reactant flow rate and the surface of the porous zone in the membrane, the design of the system would have to be optimised in order to minimise the F_R/S_p ratio and improve the yield in the reaction. In order to design an efficient reactor–separator system, the reactor should be sized by taking into account several parameters: the permeation rate of the membrane and its selectivity, the volume of the reaction zone in regard to the membrane surface in contact with it, and the catalyst load in the reactor and its distribution along the permeation zone. The reaction conditions should be also optimised to obtain a maximum yield by finding a compromise between the reduction of the reactant feed rate in relation to the membrane permeance and the amount of catalyst loaded, and the increase in the sweep gas flow in countercurrent mode.

The conditions used in this study are far from those that would be of interest for practical application. However, the exposed analysis tries to establish the basis for the design of a reactor–separator system operating under optimum conditions. Even when the use of a 100% H_2 permselective membrane is desirable for obtaining pure hydrogen for ulterior applications (i.e., fuel cell anode feeding), it has been shown that a less selective porous membrane ($\alpha_{H_2/MCH} = 15.4$) also permits considerable conversion enhancement of interest for the application of this process as an alternative for H_2 storage. By considering the fact that palladium-based membranes require operation at temperatures higher than 573 K to maintain their H_2 selectivity and to avoid the formation of pinholes by transformation of the α-PdH phase to the β phase (38, 39), the use of porous Vycor membranes in this process taking place at lower temperatures appears to be a good choice. Finally, it should be noted that after more than 100 h of continuous operation of the reactor no modification in the permeation properties of Vycor was observed.

4. CONCLUSIONS

The applicability of porous Vycor glass to a membrane reactor for the dehydrogenation of methylcyclohexane has been studied. Permeability measurements through the membrane indicate that the transport mechanism for light gases obeys the Knudsen-type diffusion model. On the other hand, the higher separation factors found for toluene (TOL) and methylcyclohexane (MCH) than for those predicted by Knudsen diffusion reveal that these compounds, and especially MCH, interact with the porous structure of the membrane and decrease their permeance compared to that of H_2, favouring their separation. The MCH dehydrogenation reaction was carried out with a Pt/Al_2O_3 catalyst, for which only TOL and H_2 were obtained as reaction products at temperatures below 523 K. The experimental conditions used in the membrane reactor largely influenced the reaction progress. The effect of several parameters on the conversion level has been explored, i.e., the reactant feed flow rate, the purge gas flow, rate, the direction of the sweep gas stream with reference to the feed flow, and the amount and distribution of the catalyst. For the permeability and selectivity values of the Vycor membrane, the best reaction conditions are achieved by minimising the ratio between the feed flow and the porous surface area and increasing the sweep gas flow rate in the countercurrent mode. The presence of a prereactor, which allows the reaction mixture to reach the membrane zone under equilibrium conditions, limits the permeation of reactant, increases the partial pressure of products all along the porous zone, and improves the net yield in the system.

APPENDIX

D_a	Damkoehler number (−), $D_a = \pi \cdot R_r^2 \cdot L \cdot \psi \cdot k_0 \cdot p_T^r / F^0_{MCH}$.
F^o_{MCH}	Molar feed rate of MCH ($mol \cdot s^{-1}$)
F_R	Reactant molar feed rate ($mol \cdot s^{-1}$)
k_0	Rate constant at inlet conditions ($mol \cdot m^{-3} \cdot s^{-1} \cdot Pa^{-1}$).
L	Reactor length (m)
p_T^r	Total pressure at the reaction side (Pa)
p^s	Pressure at the sweep side (Pa)
P_e	Peclet number (−), $P_e = F^0_{MCH}/2 \cdot \pi \cdot R_s \cdot L \cdot P_{MCH} \cdot p^s$
p_{PMCH}	MCH partial pressure (−)
P_{MCH}	MCH permeance ($mol \cdot m^{-2} \cdot s^{-1} \cdot Pa^{-1}$)
R_r	Inner ratio of the membrane (reaction side) (m)
R_s	Outer ratio of the membrane (sweep side) (m)
S_p	Porous surface (m^2)
T_1	Catalytic bed temperature (K)
T_2	Furnace temperature (K)
ψ	Catalyst loading, fraction of catalyst per volume unit at the reaction side (−).

ACKNOWLEDGMENTS

This work was supported by CICYT, Spain, under Projects MAT 1999-1005, MAT 1999-1867-E, and MAT 2000-0043-P4-03. P.F.-A. gratefully acknowledges the *Comunidad de Madrid* (Spain) for a postdoctoral fellowship.

REFERENCES

1. Dunn, S., *Int. J. Hydrogen Energy* **24**, 1157 (1999).
2. Gretz, J., Baselt, J. P., Ullmann, O., and Wendt, H., *Int. J. Hydrogen Energy* **15**(6), 419 (1990).
3. Gaudernak, B., and Lynum, S., *Int. J. Hydrogen Energy* **23**(12), 1087 (1998).
4. Edwards, J. H., *Catal. Today* **23**, 59 (1995).
5. Breault, R. W., and Rolfe, J., *in* "Proc. of the 1998 U.S. DOE Hydrogen Program Review" (1998).
6. Northeastern Advanced Vehicle consortium (NAVC), submitted for publication.
7. Guther, V., and Otto, A., *J. Alloys Compd.* **295**, 889 (1999).
8. Gadd, G. E., Blackford, M., Moricca, S., Webb, N., Evans, P. J., Smith, A. M., Jacobson, G., Leung, S., Day, A., and Hua, Q., *Science* **277**, 933 (1997).
9. De Jong, K. P., and Geus, J. W., *Catal. Rev.–Sci. Eng.* **42**(4), 481 (2000).
10. Newson, E., Hueter, Th., Hottinger, P., Von Roth, F., Scherer, G. W. H., and Schucan, Th. H., *Int. J. Hydrogen Energy* **23**(10), 905 (1998).
11. Grünenfelder, N. F., and Schucan, T. H., *Int. J. Hydrogen Energy* **14**(8), 579 (1989).
12. Scherer, G. W. H., Newson, E., and Wokaun, A., *Int. J. Hydrogen Energy* **24**, 157 (1999).
13. Klvana, D., Touzani, A., Chaouki, J., and Bélanger, G., *Int. J. Hydrogen Energy* **16**(1), 55 (1991).
14. Stanislaus, A., and Cooper, B. H., *Catal. Rev.–Sci. Eng.* **36**(1), 75 (1994).
15. Armor, J. N., *Appl. Catal. A* **222**, 91 (2001).
16. Shinji, O., Misono, M., and Yoneda, Y., *Bull. Chem. Soc. Jpn.* **55**(9), 2760 (1982).
17. Itoh, N., *AIChE J.* **33**(9), 1576 (1987).
18. Ali, J. K., Newson, E. J., and Rippin, D. W. T., *Chem. Eng. Sci.* **49**(13), 2129 (1994).
19. Okubo, T., Haruta, K., Kusakabe, K., Morooka, S., Anzai, H., and Akiyama, S., *Ind. Eng. Res.* **30**, 614 (1991).

20. Ali, J. K., and Baiker, A., *Appl. Catal. A* **155**, 41 (1997).
21. Armor, J. N., *J. Membr. Sci.* **147**, 217 (1998).
22. Terry, P. A., Anderson, M., and Tejedor, I., *J. Porous Mater.* **6**(4), 267 (1999).
23. Dittmeyer, R., Höllein, V., and Daub, K., *J. Mol. Catal. A* **173**, 135 (2001).
24. Gryaznov, V. M., Ermilova, M. M., and Orekhova, N. V., *Catal. Today* **67**, 15 (2001).
25. Ferreira-Aparicio, P., Guerrero-Ruiz, A., and Rodríguez-Ramos, I., *J. Chem. Soc. Faraday Trans.* **93**(19), 3563 (1997).
26. Elmer, T. H., "Porous and reconstructed Glasses. Engineered Materials Handbook," Vol. 4. ASM International, Materials Park, 1992.
27. Anderson, J. R., Structure of metallic catalysts. Academic Press, p. 296 (1975).
28. Ali, L. I., Ali, A.-G. A., Aboul-Fotouh, S.-M., and Aboul-Gheit, A. K., *Appl. Catal. A* **177**, 99 (1999).
29. Rouabah, D., and Fraissard, J., *J. Catal.* **144**, 30 (1993).
30. Barin, I., and Knacke, O., "Thermochemical Properties of Inorganic Substances." Springer-Verlag, Berlin/New York, 1973.
31. Tschudin, S., Shido, T., Prins, R., and Wokaun, A., *J. Catal.* **181**, 113 (1999).
32. Oyama, S. T., Lee, D., Sugiyama, S., Fukui, K., and Iwasawa, Y., *J. Mater. Sci.* **36**, 5213 (2001).
33. Tsapasis, M., and Gavalas, G., *J. Membr. Sci.* **103**, 211 (1995).
34. Prahbu, A. K., Liu, A., Lovell, L. G., and Oyama, S. T., *J. Membr. Sci.* **177**, 83 (2000).
35. Moon, W.-S., and Park, S.-B., *J. Membr. Sci.* **170**, 43 (2000).
36. Kikuchi, E., Nemoto, Y., Kajiwara, M., Uemiya, S., and Kojima, T., *Catal. Today* **56**, 75 (2000).
37. Ciavarella, P., Casanave, D., Moueddeb, H., Miachon, S., Fiaty, K., and Dalmon, J.-A., *Catal. Today* **67**, 177 (2001).
38. Uemiya, S., Kude, Y., Sugino, K., Sato, N., Matsuda, T., and Kikuchi, E., *Chem. Lett.* 1687 (1988).
39. Mardilovich, P. P., She, Y., Ma, Y. H., and Rei, M. H., *Separations* **44**(2), 310 (1998).